New techniques for wave-field rendering of polygon-based high-definition CGHs

doi: 10.1117/12.876362

New techniques for wave-field rendering of polygon-based high-definition CGHs

Hirohito Nishi[a], Kentaro Higashi[a], Yasuaki Arima[a], Kyoji Matsushima[a] and Sumio Nakahara[b]

[a]Department of Electrical and Electronic Engineering
[b]Department of Mechanical Engineering
Kansai University, Yamate-cho 3-3-35, Suita, Osaka 564-8680, Japan

ABSTRACT

Four novel techniques are introduced into polygon-based high-definition CGHs (PBHD-CGH) that feature the true-fine spatial 3D image accompanied with a strong sensation of depth. The first is algorithm for creating specular surfaces based on Phong reflection model. This is very useful for providing a feel of material to polygonal surfaces. The second technique is called digitized holography that replaces the entire processes of classical holography by their digital counterparts. The wave-field of real-existent objects can be optically reconstructed by the digitized holography. This technique makes it possible to edit the 3D scene of holograms or create mixed 3D scene of the real and virtual objects. Another technique for creating PBHD-CGH of real-existent objects is also proposed by a CG-like method using a 3D laser scanner that measures the 3D shape of the object. Finally, a prototype PBHD-CGH is demonstrated for creating landscape scenery. This CGH is intended to reconstruct a scene as if the viewers see mountain scenery through the window given by the CGH.

Keywords: Computer-generated hologram, Polygon-based method, Specular surface, Texture-mapping, Digitized holography, 3D scan, Synthetic aperture digital holography

1. INTRODUCTION

Spatial 3D images optically reconstructed by full-parallax high-definition computer-generated holograms (HD-CGH) are very different from that by conventional 3D systems. The full-parallax HD-CGHs give viewers a strong sensation of depth that never has been caused by the conventional systems providing only binocular disparity. Recently, we reported a set of techniques to create full-parallax HD-CGHs with more than billions pixels, which be able to reconstruct occluded 3D scenes constructed of surface-modeled object.[1–4] These CGHs are created by techniques based on the polygon method[5] for generating object fields and the silhouette method[3,14,15] for light-shielding. Therefore, the HD-CGHs are called polygon-based high-definition CGHs (PBHD-CGH).[6]

In the last meeting, we also introduced a new technique for field propagation, named shifted angular spectrum method,[7] into creation of PBHD-CGHs.[6,8] Since this numerical technique removes any constraints on field propagation, PBHD-CGHs gain the freedom of arrangement of the objects in the 3D scenes.

One of advantages of the polygon-based method is similarity to conventional computer graphics based on polygon models. Techniques of texture-mapping and smooth shading used in CG such as Gouraud and Phong shading are successfully introduced into PBHD-CGHs and put more expression into the reconstructed 3D images.[6,9,10] We call these techniques wave-field rendering.

In this paper, we propose some other rendering techniques for PBHD-CGHs. First, we present a new algorithm to give metal-like specular surfaces to CG-modeled virtual objects. This is a very important technique to produce a feel of material of the reconstructed objects. Second, we present techniques to create 3D images of real-existent objects. Two techniques are proposed for this purpose: One is the use of a 3D scanner and another is digitized holography. The former is a conventional CG-like technique; the photograph of the real object is texture-mapped onto the 3D-meshed object whose mesh data is measured by using a 3D laser scanner. The latter is a little evolutionary; the fields of real-existent objects are widely captured by using the technique of synthetic aperture

Further author information: (Send correspondence to K. Matsushima)
E-mail: matsu@kansai-u.ac.jp

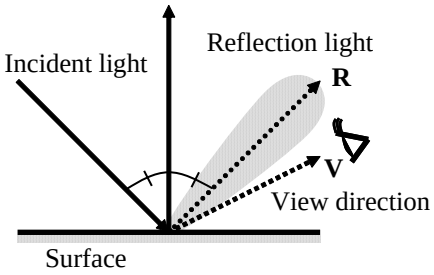

Figure 1. Phong reflection model.

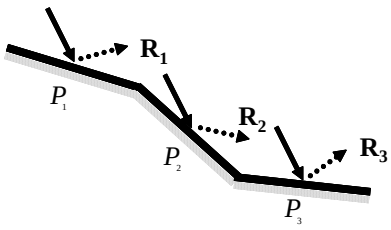

Figure 2. Reflection in polygonal surfaces.

digital holography.[11] We call this technique digitized holography, because this is the technique completely replacing classical holography by a modern digital way. Finally, we introduce an attempt to create CGHs that reconstruct mountain scenery as if viewers see a landscape through the window of the CGH.

2. RENDERING FACETED SPECULAR SURFACES

2.1 Spectral envelope of specular surface function based on Phong reflection model

In the polygon-based method, 3-D objects is composed of many polygons. Each polygon is regarded as a planar surface source of light whose shape is polygonal. The surface sources are expressed by complex functions referred to as a surface function. The common form of the surface function is given by:

$$h(x, y) = a(x, y) \exp[i\phi(x, y)], \tag{1}$$

where the amplitude distribution $a(x, y)$ gives the shape, texture, and brightness of the polygon, while the phase distribution $\phi(x, y)$ provides diffusiveness of light. A specular surface obviously has a limited diffusiveness in contrast with the diffused surfaces. Therefore, the spectrum of the surface functions must be band-limited in specular surfaces. We make use of Phong model to determine the spectral envelope of phase distribution $\phi(x, y)$. Phong reflection model is the most popular model for rendering a specular surface in CG. According to Phong model, the brightness observed in a view point is given as:

$$I(\mathbf{V}, \mathbf{R}) = k_s(\mathbf{R} \cdot \mathbf{V})^{\alpha}, \tag{2}$$

where k_s and α are a specular reflection and shininess constant, respectively. The vector $\mathbf{R} = (R_x, R_y, R_z)$ gives the reflection direction, whereas the vector $\mathbf{V}$ gives the viewer direction, as illustrated in Fig. 1. Supposing that the view direction can be interpreted as the unit wave vector of a plane wave, $\mathbf{V}$ is given as:

$$\mathbf{V} = \lambda(u, v, (\lambda^{-2} - u^2 - v^2)^{1/2}), \tag{3}$$

where u and v are Fourier frequencies with respect to x and y direction. Substituting Eq. (3) into (2), the envelope of spectrum of the phase distribution is obtained as following:

$$\begin{aligned} A_s(u, v, \mathbf{R}) &= I(\mathbf{V}, \mathbf{R})^{1/2} \\ &= k_s^{1/2}[\lambda(R_x u + R_y v + R_z(\lambda^{-2} - u^2 - v^2)^{1/2})]^{\alpha/2}. \end{aligned} \tag{4}$$

To give a Phong-modeled specular surface to the object, the phase distribution $\phi(x, y)$ should be modified so that its spectral envelope is fitted to the $A_s(u, v, \mathbf{R})$. In this study, iterative Fourier-transform algorithm (IFTA)[12] is used for the modification of the spectral envelope of the diffusive phase.

In the IFTA, The surface function is first Fourier-transformed into spectrum and then only the amplitude distribution of the spectrum is deformed so that the spectral envelope corresponds with the $A_s(u, v, \mathbf{R})$. The deformed spectrum is then transformed back to the complex amplitude in the real space in that only the amplitude distribution is deformed again so that the amplitude distribution corresponds with the polygonal surface. The iteration of this procedure generates the surface function of the specular surface whose spectral envelope agrees with $A_s(u, v, \mathbf{R})$.

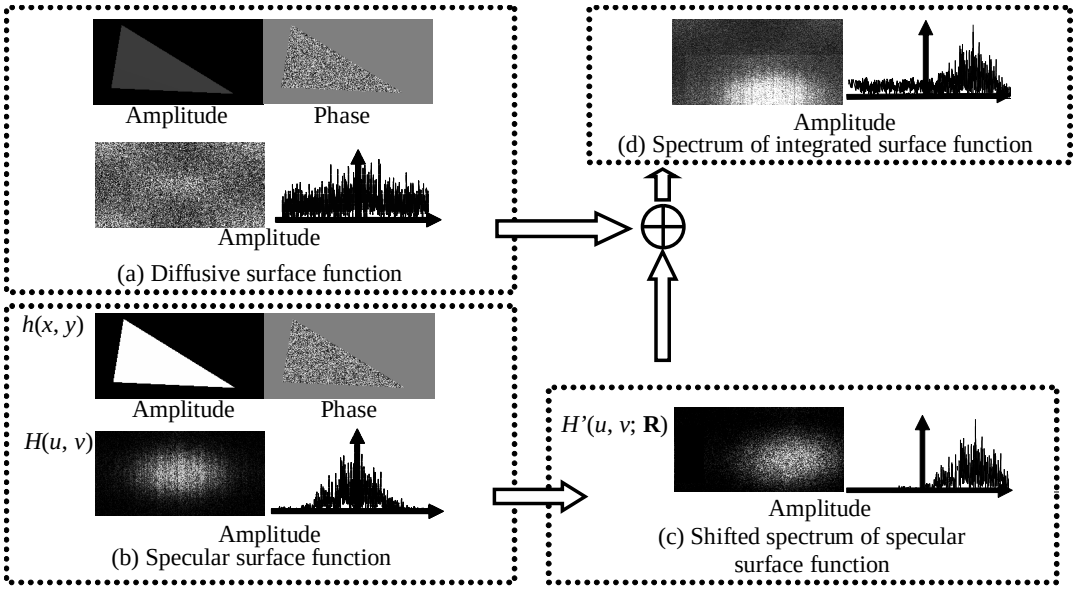

Figure 3. An example of the procedure for generating specular surfaces.

2.2 Rendering object composed of specular surfaces

A specular polygon is created by the method based on the IFTA and Phong reflection model in the previous section. However, the method is too time-consuming to calculate the wave-field of an object composed of many polygons. Each polygon composing the object has its own reflection vector of $\mathbf{R}$ as shown in Fig. 2. Therefore, the procedure for the IFTA that involves many iterations of Fourier transform must be performed for each polygon. This is the reason why the method is expected to be much time-consuming.

We adopt shifting carrier frequency of the spectrum in order to avoid unnecessary repeat of the IFTA. At the beginning, a complex function $g(x, y)$ is generated by the method in section 2 using the reflection vector of $\mathbf{R} = (0, 0, 1)$. Here, the amplitude of the function is a constant of unity, i.e. $|g(x, y)| \equiv 1$. Therefore, this complex function is not a surface function but a phase-modulated function given as the following form:

$$g(x, y) = \exp[i\phi'(x, y)]. \tag{5}$$

The surface function of a specific polygonal surface is provided by using the phase-modulated function as follows:

$$h(x, y) = a(x, y)g(x, y), \tag{6}$$

where $a(x, y)$ gives the shape of polygon again. The surface function $h(x, y)$ gives a limited diffusiveness based on Phong model, in which the reflection light mainly travels in the normal direction of the surface. To force the light to travel in arbitrary direction given by $\mathbf{R}$, the function $h(x, y)$ is multiplied by the wave-field of a plane-wave traveling in the direction of $\mathbf{R}$ as follows:

$$h'(x, y; \mathbf{R}) = h(x, y) \exp[ik\mathbf{R} \cdot \mathbf{r}], \tag{7}$$

where k is the wavenumber and thus $\exp[ik\mathbf{R} \cdot \mathbf{r}] = \exp[ik(R_x x + R_y y)]$ is the plane wave traveling into the $\mathbf{R}$ direction. Equation (7), however, usually causes an aliasing error for the sampling interval of the given (x, y) grid. In the Fourier space, Eq. (7) means that the spectrum $H(u, v) = F\{h(x, y)\}$ is shifted as follows:

$$\begin{aligned} H'(u, v; \mathbf{R}) &= F\{h'(x, y; \mathbf{R})\} \\ &= H(u - \frac{R_x}{\lambda}, v - \frac{R_y}{\lambda}). \end{aligned} \tag{8}$$

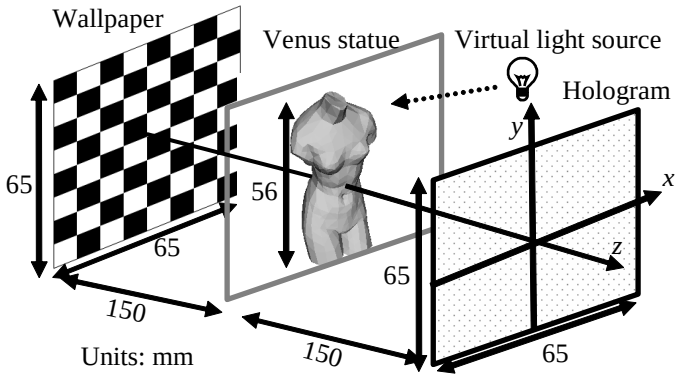

Figure 4. The 3-D scene of "The Metal Venus I".

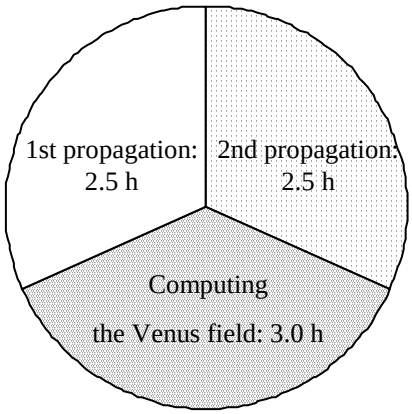

Figure 5. Itemized computation time of The Metal Venus I.

Therefore, we use the spectrum $H'(u, v; \mathbf{R})$ instead of using Eq. (7). As a result, the phase-modulated function $g(x, y)$ generated only once in $\mathbf{R} = (0, 0, 1)$ can be used for any direction of $\mathbf{R}$.

Figure 3 shows an example of the procedure of the proposed rendering method for generating specular surfaces. The diffusive light, whose surface function is shown in (a), should be mixed with the light produced from the specular surface function in (b) for realistic rendering, because the specular-only surfaces lead to a narrow viewing-zone. The diffusive surface function (a) is only Fourier transformed, whereas the specular surface function is Fourier-transformed and then shifted by using Eq. (8) as in (c). These two surface functions are superposed in the Fourier space, as shown in (d).

2.3 Creation of PBHD-CGH for specular object

We created a PBHD-CGH named "The Metal Venus I" after the first PBHD-CGH "The Venus" with a diffusive surface.[3] The 3D scene of the CGH illustrated in Fig. 4 is almost the same as that of The Venus. The statue of the Venus is 5.6 cm in height and composed of 1396 polygons. Parameters used for computing the CGH are summarized in Table 1.

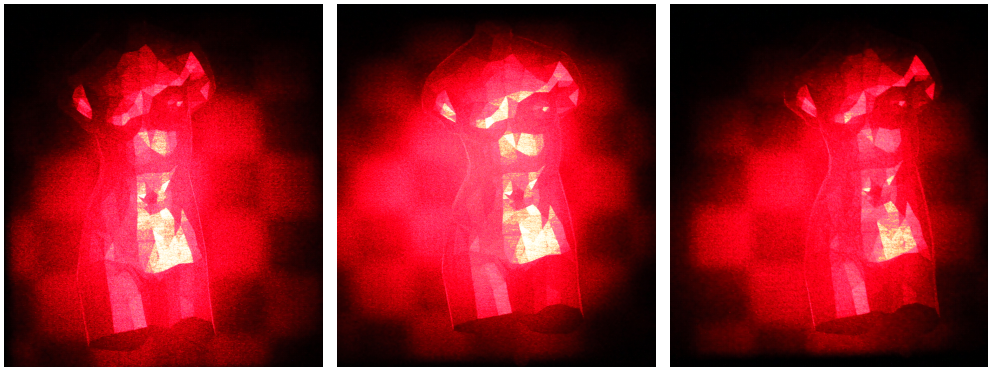

(a) Left (b) Center (c) Right

Figure 6. Photographs of optical reconstructs of The Metal Venus I. The photographs (a)–(c) are taken from different view-points.

Computation of the CGH was executed by using a PC with four CPUs of the Xeon E7330 (2.4 G Hz) and memory of 96 G bytes. The total computation time was approximately 8.0 h. The itemized computation time is shown in Fig. 5. The longest time was consumed by computation of the object (Venus statue) field. This is 1.5 times longer than the original Venus rendered only with diffusive surfaces*, because specular fields are separately computed and then added to the diffusive field.

Figure 6 shows the optical reconstruction of The Metal Venus I. It is verified that the surface brightness is changed dependently on the view point.

3. RENDERING REAL-EXISTENT OBJECTS BY DIGITIZED HOLOGRAPHY

In classical holography, the object wave of a real-existent object is recorded on light-sensitive films by interference with reference waves. Then, the object wave is reconstructed by diffraction by the fringe pattern. It is theoretically possible to replace these entire processes by their digital counterparts. In fact, the PBHD-CGHs allow us to reconstruct completely virtual 3D scenes by diffraction by the synthetic fringe pattern. This means that the latter half, i.e. reconstruction of object waves, is already realized. However, it is not easy to realize the former half, recording object wave, by using a digital manner. Although it is theoretically possible to capture any object field by using digital holography (DH), currently available image sensors, in practice, do not meet the requirement of PBHD-CGHs such as pixel sizes and pitches, which make it possible to reconstruct true fine 3D images.

To resolve the problem, we use the technique of lensless-Fourier synthetic-aperture digital holography (LFSA-DH).[11]This is a type of DH using a spherical reference wave and makes it possible to replace the whole process of the classical holography with digital signal processing (DSP) of optical wave fields. We refer to this technique as digitized holography. The digitized holography allows us to digitally edit, archive, transmit, and optically reconstruct the wave-field of real-existent 3D objects.

In this section, we report a PBHD-CGH created as digitized holography. The CGHs, named "Bear II" optically reconstruct mixed 3D scenes including CG-modeled 3D objects, 2D digital images, and multiple real-existent objects whose field is captured by using the LFSA-DH.

3.1 Principle for reducing sampling intervals and increasing sampling cross section

In the LFSA-DH, the wave-field of an object is obtained by Fourier transform of the captured field. The sampling intervals of the Fourier-transformed wave-field are given by the following equation in the image plane:[11]

$$\Delta_x = \frac{\lambda d_R}{N_x \delta_x}, \qquad \Delta_y = \frac{\lambda d_R}{N_y \delta_y}, \tag{9}$$

where λ and d_R are the wavelength and the distance between the center of the spherical reference wave and the image sensor. Number of the sensor pixels and the sensor pitches are $N_x \times N_y$ and $\delta_x \times \delta_y$, respectively.

Since the sampling intervals are reduced with increasing the sensor pixels, the technique of the synthetic aperture is used for increasing the effective number of the pixels.[13] In the synthetic aperture DH, the image sensor is mechanically translated and captures the wave field at different positions. Here, an amount of the sensor shift is set to be smaller than the sensor area in order to overlap the captured field at each position. This overlap area is used for avoiding translation errors and obtaining exact sensor position by use of a correlation function between the captured fields.[13] As a result, it is possible to integrate all captured fields into a large-scaled wave field.

*According to the early paper, computation time for the object (Venus statue) was 7.6 h.[3] However, the time has been reduced by the improvement of the implement and use of more powerful PCs.

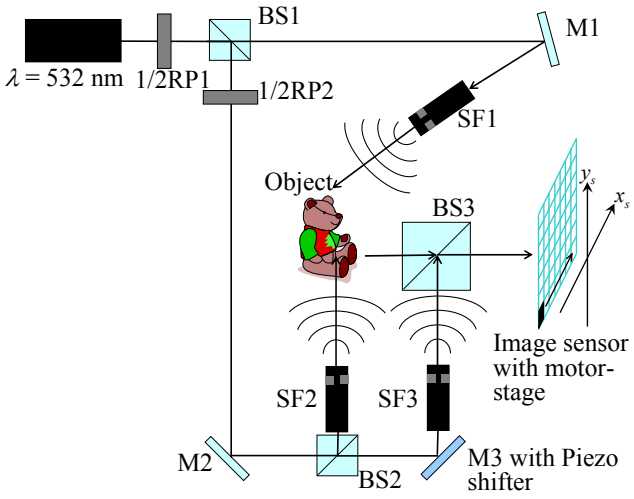

Figure 7. Experimental setup for capturing a large wave-field by synthetic aperture digital holography. M: mirror, BS: beam splitter, RP: retarder plate.

3.2 Experiment for capturing large-scaled wave-fields by LFSA-DH

The experimental setup for capturing large-scaled wave-fields by the LFSA-DH is shown in Fig. 7. The image sensor with 3000 × 2200 pixels (Lumenera Lw625) is mechanically translated by a PC-controlled motor-stage. The fringe pattern is captured 3 times for each position to obtain a complex wave-field using the phase-shift caused by the mirror M3 installed in a Piezo phase-shifter.

Amplitude image of the captured and Fourier-transformed field are shown in Fig. 8 (a) and (b), respectively. The total field is obtained by stitching individual fields captured at 8 × 12 positions. The total cross section of the captured field is $77 \times 80\text{mm}^2$. Here, the distance d_R between the reference point source provided by SF3 and the sensor plane is 21.5 cm. This distance is a free parameter and thus determined so that the sampling intervals of the Fourier-transformed field is $1.0\mu\text{m} \times 1.0\mu\text{m}$.

3.3 CGH for mixed 3D scene including virtual and real objects

3.3.1 Mixed 3D scene

The real-existent object, the ornament of a small bear whose wave-field is capture by the LFSA-DH, is mixed with the virtual 3D scene. The design of the scene is shown in Fig. 9. Here, the bear appears twice on the scene, i.e. the same captured wave-field is used twice in the scene. This is impossible in classical holography. Only digitized holography allows us to edit the 3D scene. Some virtual objects such as 2D wallpaper or 3D bees are arranged behind or in front of a double bear.

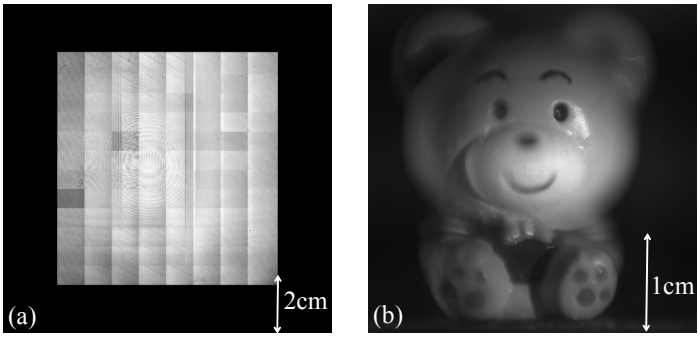

Figure 8. Amplitude images of the captured (a) and Fourier-transformed field (b).

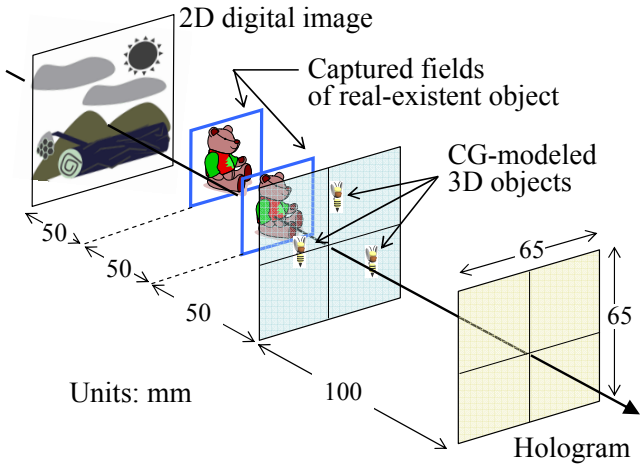

Figure 9. The mixed 3D scene of "Bear II" including the field of the real-existent object and the CG-modeled virtual object.

3.3.2 Light-shielding by silhouette method

The light behind the real-existent object must be shielded to prevent the object from being a phantom image and correctly reconstruct the occluded scene. The silhouette method[3, 14, 15] proposed for light-shielding in synthetic holography is applied to the real-existent object. The principle of light-shielding in captured fields is shown in Fig. 10. Since the incident field behind the captured object should be shielded over the cross section of the object, the incident field is multiplied by a binary mask that corresponds with the silhouette of the object. Then, the captured field is added to the masked field. The silhouette-mask image used is shown in Fig. 11 (b). This image is produced from the amplitude image of (a) that is obtained from a small part of the captured field to avoid blur.

3.3.3 Fabrication and reconstruction of "Bear II"

The number of pixels of the Bear II is approximately 4 G pixels ($\cong 65,536 \times 65,536$). Since the pixel pitches are 1.0 μm$\times$ 1.0 μm, the viewing angle is 37° both in horizontal and vertical. The parameters used are summarized in Table 1. After calculation of the total wave-field of the scene including captured fields, the fringe pattern is generated by numerical interference with the reference wave, and then quantized to produce the binary pattern. Finally, the binary amplitude hologram is fabricated by using laser lithography system.

Photographs of the optical reconstruction of the Bear II are shown in Fig. 12. It is verified that occlusion of the 3D scene is accurately reconstructed, because the appearance of the 3D scene varies when the point of view changes.

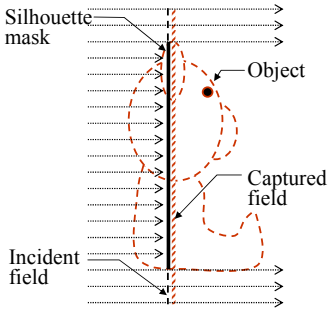

Figure 10. The principle of the silhouette method in captured fields.

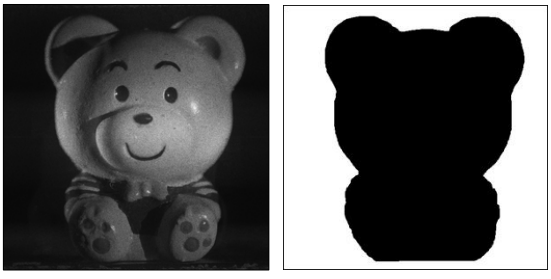

(a) Amplitude image (b) Silhouette mask

Figure 11. (a) The amplitude image obtained from a small part of the captured field. (b) The silhouette mask produced from the amplitude image.

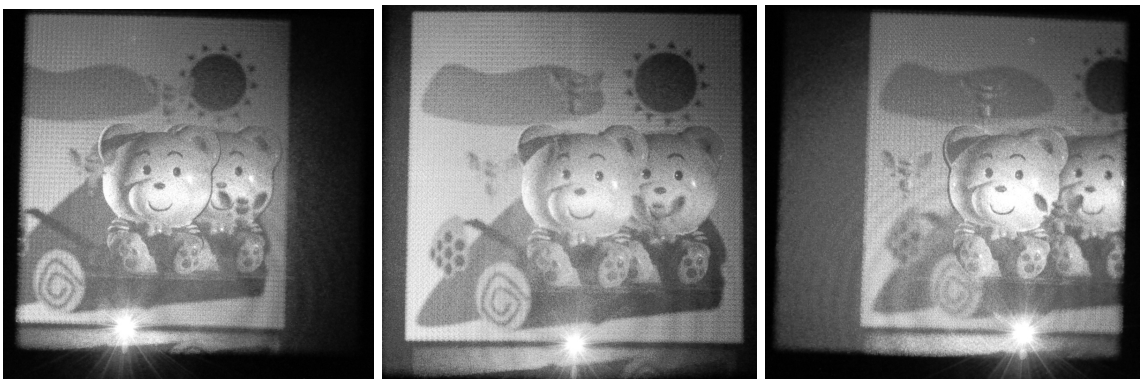

(a) Left (b) Center (c) Right

Figure 12. Photographs of optical reconstruction of the "Bear II" created for the mixed 3D scene including real-existent and virtual objects. Photographs (a) – (c) are taken from different view points.

4. RENDERING REAL-EXISTENT OBJECTS BY 3D LASER SCANNER

In holography, the object wave emitted from a real-existent object that is illuminated by coherent light is recorded by optical interference with reference waves. However, recording real-existent objects without illumination by coherent light sometimes has an advantage. For example, a real building can not be recorded by holography, because the object is too large to be illuminated by coherent light. In this section, CG-like approach is presented for recording and reconstructing real-existent 3D objects by using PBHD-CGHs.

4.1 Measurement of 3D objects by using 3D scanner

The shape of 3D objects are measured by a 3D laser scanner, Konica Minolta Vivid 910. This equipment is able to scan a 3D object in 2.5 s and output its 3D shape as polygon mesh data. The measurement error is less than ±0.05m in all directions. The Vivid 910 also has a function of capturing the in-line digital image of the object. Since the polygon method is similar to CG as mentioned above, the digital 2D image can be used for texture-mapping[6,16] in order to produce more realistic 3D images.

Here, live faces are chosen as the object recorded by the 3D scanner and reconstructed by PBHD-CGHs, because it is not easy to record live faces by conventional holography. Figure 13 shows snapshots of the scene of 3D measurement of live faces. The CG image rendered by texture-mapping onto the polygon mesh is also shown in Fig. 14

4.2 Fabrication and reconstruction of the PBHD-CGHs

The polygon-meshed object with 2822 polygons is placed at 10 cm behind the hologram plane. The wallpaper made by 2D digital image is also arranged at 12 cm behind the polygon-meshed object to enhance the depth

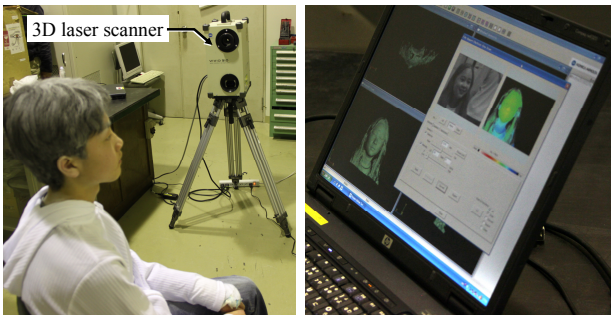

Figure 13. Snapshots of measurement of the 3D shape of live faces by using the 3D laser scanner.

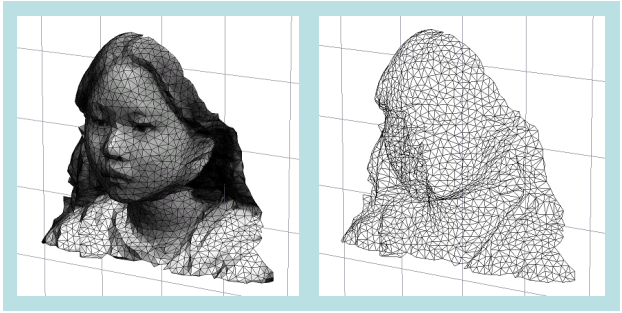

Figure 14. Computer graphics of the measured polygon mesh data.

(a) Left (b) Center (c) Right

Figure 15. Photographs of optical reconstruction of the fabricated PBHD-CGH. Photographs are taken from different view-points.

sensation. Number of pixels of the calculated and fabricated PBHD-CGH is $131,072 \times 65,536$ pixels. Since the pixel pitched are 0.8 μm both in horizontal and vertical direction, the viewing-angles are approximately 45° in both directions.

Figure 15 shows the optical reconstruction. The reconstructed 3D image is certainly a 3D portrait.

5. RENDERING MOUNTAIN SCENERY

The PBHD-CGH described in this section is intended to reconstruct a scene as if viewers see mountain scenery through a window. Since the CGH plays a role of the window, the perspective through the window should vary with change of the viewpoint. Furthermore, the terrain beyond the window should extend as far as viewers can see.

There are mainly two problems to create the intended CGH. One is how to calculate the wave-field of a very big and uninterrupted object. This is most likely very time-consuming. Another problem is how to prevent the reconstructed 3D scene from be a phantom image. The object model for mountain scenery commonly has self-occlusion. The silhouette method is used for creating PBHD-CGHs of occluded scenes. In this technique, the wave-field behind the object is shielded by the mask obtained from the silhouette of the object. This technique makes it possible to create mutual occluded 3D scenes. However, if an object has self occlusion, the object may be reconstructed as a partial phantom image, because the light-shielding is made for object by object at this stage. If light is shielded polygon by polygon, self-occlusion can be correctly reconstructed. However, this technique is too time-consuming to create HD-CGHs whose number of pixels reach to billion pixels.

Figure 16 is the 3D scene of the prototype CGH "Moutain" reconstructing mountain scenery. The parameters are shown in Table 1. To resolve the problem mentioned above, we split the object model into several sub-objects and insert several masks between the sub-objects as shown in Fig. 17. Here, the inserted masks correspond to

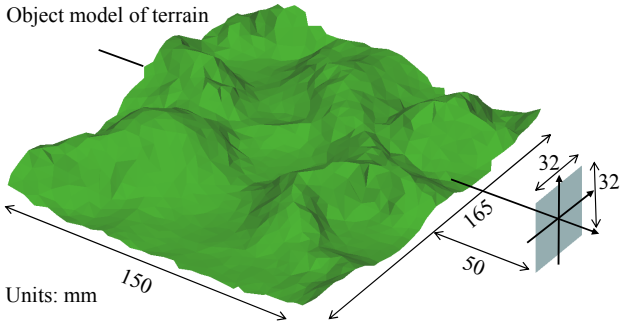

Figure 16. The 3D scene of the prototype CGH reconstructing mountain scenery.

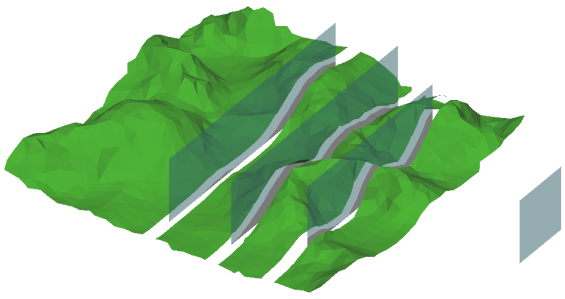

Figure 17. Schematic illustration of splitting and masking the object.

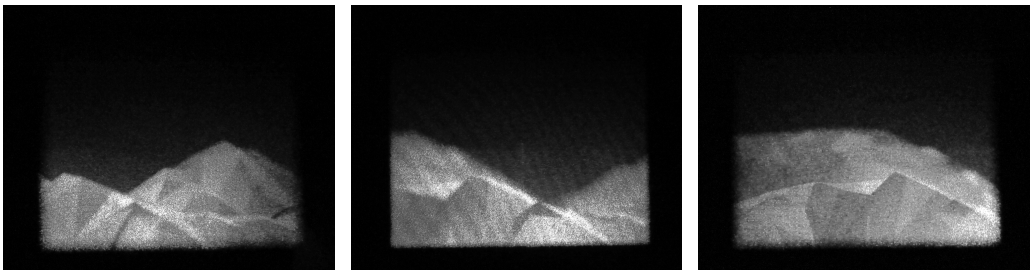

(a) Left (b) Center (c) Right

Figure 18. Photographs of optical reconstruction of the prototype CGH. Photographs (a) – (c) are taken from different view-points.

the shape of cross section of the terrain model. Unfortunately, the positions where masks should be inserted and necessary number of masks are determined a priori at this stage.

The optical reconstruction is shown in Fig. 18. It is verified that the mountain scenery is reconstructed as intended.

6. CONCLUSION

Several techniques are newly and successfully introduced into full-parallax polygon-based high-definition CGHs. The parameters of the created CGHs are summarized in Table 1. These new techniques are expected to enhance power of expression of spatial 3D images reconstructed by full-parallax PBHD-CGHs.

ACKNOWLEDGMENTS

The authors thank Prof. Kanaya for his assistance in 3D scan of live faces. The mesh data for the Venus object is provided courtesy of INRIA by the AIM@SHAPE Shape Repository. This work was supported by the JSPS.KAKENHI (21500114).

REFERENCES

[1] Matsushima, K. and Nakahara, S., "Region segmentation and parallel processing for creating large-scale CGHs in polygon source method," *Proc. SPIE* **7233**, 72330E (2009).

Table 1. Summary of parameters of created PBHD-CGHs.

Name		The Metal Venus I	Bear II	Shion	Mountain
Feature		Specular surface	Digitized holography	3D scan	Mountain scenery
Number of pixels [a]		64K × 64K	64K × 64K	128K × 64K	32K × 32K
Pixel pitches	μm × μm	1.0 × 1.0	1.0 × 1.0	0.8 × 0.8	1.0 × 1.0
Hologram size	mm^2	65.5 × 65.5	65.5 × 65.5	105 × 52.4	32.8 × 32.8
Wavelength	nm	633	532	633	633
Number of polygons [b]		718	N.A.	2822	919
Computation time	hour	8.0 [c]	N.A.	8.6 [d]	23.0 [c]

[a] 1K = 1024

[b] front-surface only

[c] CPU : XEON E7330 (2.4 G Hz) × 4 (Total 16 processor cores) / Memory : 96 G Bytes

[d] CPU : XEON E7540 (2.0 G Hz) × 4 (Total 24 processor cores) / Memory : 256 G Bytes

[2] Matsushima, K. and Nakahara, S., "A high-definition full-parallax cgh created by the polygon-based method," *OSA Topical Meeting on Digital Holography and Three-Dimensional Imaging* , PDWB38 (2009).

[3] Matsushima, K. and Nakahara, S., "Extremely high-definition full-parallax computer-generated hologram created by the polygon-based method," *Appl. Opt.* **48**, H54–H63 (2009).

[4] Matsushima, K., Nishi, H., Arima, Y., Higashi, K., Nakamura, M., and Nakahara, S., "Impact of spatial 3D imaging by extremely high-definition computational holography," *17th Int. Display Workshop (IDW '10)* **2**, 1333–1334 (2010).

[5] Matsushima, K., "Computer-generated holograms for three-dimensional surface objects with shade and texture," *Appl. Opt.* **44**, 4607–4614 (2005).

[6] Matsushima, K., Nakamura, M., and Nakahara, S., "Novel techniques introduced into polygon-based high-definition CGHs," *OSA Topical Meeting on Digital Holography and Three-Dimensional Imaging* , JMA10 (2010).

[7] Matsushima, K., "Shifted angular spectrum method for off-axis numerical propagation," *Opt. Express* **18**, 18453–18463 (2010).

[8] Matsushima, K. and Nakahara, S., "High-definition full-parallax CGHs created by using the polygon-based method and the shifted angular spectrum method," *Proc. SPIE* **7619**, 761913–761921 (2010).

[9] Matsusima, K., Nakamura, M., Kanaya, I., and Nakahara, S., "Computational holography: Real 3D by fast wave-field rendering in ultra-high resolution," *SIGGRAPH 2010* (2010).

[10] Matsushima, K., "Spatial imaging based on extremely high-definition computational holography," *17th Int. Display Workshop (IDW '10)* **2**, 1237–1240 (2010).

[11] Nakatsuji, T. and Matsushima, K., "Free-viewpoint images captured using phase-shifting synthetic aperture digital holography," *Appl. Opt.* **47**, D136–D143 (2008).

[12] Bräuer, R., Wyrowski, F., and Bryngdahl, O., "Diffusers in digital holography," *J. Opt. Soc. Am.* **A8**, 572–578 (1991).

[13] Binet, R., Colineau, J., and Lehureau, J.-C., "Short-range synthetic aperture imaging at 633 nm by digital holography," *Appl. Opt.* **41**(23), 4775–4782 (2002).

[14] Matsushima, K. and Kondoh, A., "A wave optical algorithm for hidden-surface removal in digitally synthetic full-parallax holograms for three-dimensional objects," *SPIE Proc. Practical Holography XVIII* **#5290**, 90–97 (2004).

[15] Kondoh, A. and Matsushima, K., "Hidden surface removal in full-parallax CGHs by silhouette approximation," *Systems and Computers in Japan* **38**, 53–61 (2004).

[16] Matsushima, K., "Wave-field rendering in computational holography," *IEEE/ACIS 9th Int. Conf. on Computer and Information Science (ICIS 2010)* , 846–851 (2010).